

Seismic-Wave Propagation in Viscoelastic Media with Material Discontinuities: A 3D Fourth-Order Staggered-Grid Finite-Difference Modeling

by Jozef Kristek and Peter Moczo

Abstract We address the basic theoretical and algorithmic aspects of memory-efficient implementation of realistic attenuation in the staggered-grid finite-difference modeling of seismic-wave propagation in media with material discontinuities. We show that if averaging is applied to viscoelastic moduli in the frequency domain, it is possible to determine anelastic coefficients of the averaged medium representing a material discontinuity. We define (1) the anelastic functions in a new way, as being independent of anelastic coefficients, and (2) a new coarse spatial distribution of the anelastic functions in order to properly account for material discontinuities and, at the same time, to have it memory efficient. Numerical tests demonstrate that our approach enables more accurate viscoelastic modeling than other approaches.

Introduction

The principal difficulty of implementation of realistic attenuation in time-domain methods is due to the fact that the stress–strain relation has the form of a convolution integral. Day and Minster (1984) used the Padé approximation to expand a frequency-dependent viscoelastic modulus into an n th-order rational function in order to replace the convolutive integral by n first-order differential equations. Emmerich and Korn (1987) improved the approach (in terms of accuracy and efficiency) by considering the rheology of the generalized Maxwell body (GMB) whose viscoelastic modulus has the desired rational form. Carcione *et al.* (1988) developed an alternative approach based on rheology of the generalized Zener body. All the approaches allow for both an arbitrary attenuation-frequency law and its spatial heterogeneity.

In this article we consider the GMB rheology. In a Cartesian coordinate system (x_1, x_2, x_3) , let $\rho(x_i)$, $i \in \{1,2,3\}$, be density, $\kappa(x_i)$ elastic bulk modulus, $\mu(x_i)$ elastic shear modulus, $\vec{u}(x_i, t)$ the displacement vector, t time, $\vec{f}(x_i, t)$ body force per unit volume, $\tau_{ij}(x_k, t)$ and $\varepsilon_{ij}(x_k, t)$, $i, j, k \in \{1,2,3\}$, stress and strain tensors. (Further, x_1, x_2, x_3 and x, y, z will be used interchangeably.) Following Emmerich and Korn (1987), the equation of motion and Hooke’s law for an isotropic viscoelastic medium can be written as (summation convention for repeated subscripts assumed)

$$\rho \ddot{u}_i = \tau_{ij,j} + f_i \quad (1)$$

and

$$\tau_{ij} = \kappa \varepsilon_{kk} \delta_{ij} + 2\mu (\varepsilon_{ij} - \frac{1}{3} \varepsilon_{kk} \delta_{ij}) - \sum_{l=1}^n [\kappa \zeta_l^{\kappa,kk} \delta_{ij} + 2\mu (\zeta_l^{\mu,ij} - \frac{1}{3} \zeta_l^{\mu,kk} \delta_{ij})], \quad (2)$$

where $\tau_{ijj} = \partial \tau_{ij} / \partial x_j$ and anelastic functions $\zeta_l^{M,ij}$, $M \in \{\kappa, \mu\}$, $l = 1, 2, \dots, n$, satisfy $9n$ equations

$$\dot{\zeta}_l^{M,ij} + \omega_l \zeta_l^{M,ij} = \omega_l Y_l^M \varepsilon_{ij}. \quad (3)$$

(Some authors use the term “memory variables” instead of “anelastic functions.”) Here, ω_l ($l = 1, 2, \dots, n$) are the angular relaxation frequencies. The anelastic coefficients Y_l^κ and Y_l^μ are obtained from the systems of equations

$$\sum_{i=1}^n \frac{\omega_l \tilde{\omega}_k + \omega_l^2 \tilde{Q}_\eta^{-1}(\tilde{\omega}_k)}{\tilde{\omega}_k^2 + \omega_l^2} Y_l^\eta = \tilde{Q}_\eta^{-1}(\tilde{\omega}_k); \quad (4)$$

$$k = 1, \dots, 2n - 1, \eta \in \{\alpha, \beta\}$$

$$Y_l^\mu = Y_l^\beta, Y_l^\kappa = \frac{\alpha^2 Y_l^\alpha - \frac{4}{3} \beta^2 Y_l^\beta}{\alpha^2 - \frac{4}{3} \beta^2}, \quad (5)$$

where

$$\alpha = [(\kappa + \frac{4}{3} \mu) / \rho]^{1/2}, \quad (\mu / \rho)^{1/2}.$$

Here, $\tilde{Q}_\alpha(\tilde{\omega}_k)$ and $\tilde{Q}_\beta(\tilde{\omega}_k)$ are desired values of the quality factors for the P and S waves, respectively, at frequencies $\tilde{\omega}_k$. It is reasonable that both ω_l and $\tilde{\omega}_k$ cover the frequency range of interest logarithmically equidistantly, $\tilde{\omega}_1 = \omega_1$, and $\tilde{\omega}_{2n-1} = \omega_n$. The rheology of the considered viscoelastic medium is represented by two GMBs representing viscoelastic bulk and shear moduli. The rheology is schematically illustrated in Figure 1. The GMB viscoelastic modulus is

$$M_n(\omega) = M_U \left(1 - \sum_{l=1}^n Y_l^M \frac{\omega_l}{i\omega + \omega_l} \right), \quad M_U \in \{\kappa, \mu\}, \quad (6)$$

where the subscript U indicates the unrelaxed modulus. (Note that in practice phase velocities at certain frequencies are usually known. Relations between the phase velocities and corresponding unrelaxed moduli can be found in Moczo *et al.* [1997].)

In order to reduce the number of the anelastic functions from $9n$ to $6n$, we can rewrite equations (2) and (3) as

$$\tau_{ij} = \kappa \varepsilon_{kk} \delta_{ij} + 2\mu \left(\varepsilon_{ij} - \frac{1}{3} \varepsilon_{kk} \delta_{ij} \right) - \sum_{l=1}^n \zeta_l^{ij} \quad (7)$$

and

$$\dot{\zeta}_l^{ij} + \omega_l \zeta_l^{ij} = \omega_l \left[\kappa Y_l^K \varepsilon_{kk} \delta_{ij} + 2\mu Y_l^\mu \left(\varepsilon_{ij} - \frac{1}{3} \varepsilon_{kk} \delta_{ij} \right) \right], \quad l = 1, 2, \dots, n \quad (8)$$

using modified anelastic functions ζ_l^{ij} . Simple implementation of the attenuation in the displacement-stress or displacement-velocity-stress or velocity-stress finite-difference (FD) schemes (for the schemes see, e.g., Graves [1996], Moczo *et al.* [2001], and Moczo *et al.* [2002]) yields additional (in respect to the perfectly elastic case) quantities in each grid cell:

$$Y_l^K, Y_l^\mu, Y_l^{\mu_{xy}}, Y_l^{\mu_{yz}}, Y_l^{\mu_{zx}}, \zeta_l^{xx}, \zeta_l^{yy}, \zeta_l^{zz}, \zeta_l^{xy}, \zeta_l^{yz}, \zeta_l^{zx}, \quad l = 1, 2, \dots, n. \quad (9)$$

Location of the anelastic functions and coefficients in the staggered-grid cell is shown in Figure 2. Note that heterogeneity of the medium inside the cell itself is assumed. The corresponding number of bytes of additional memory in the $MX \cdot MY \cdot MZ$ rectangular grid is

$$N^{\text{additional}} = p \cdot MX \cdot MY \cdot MZ \cdot 11 \cdot n, \quad (10)$$

where $p = 4$ or 8 in single or double precision, respectively. Because n should be at least 3, the total additional memory obviously is very large.

The number of anelastic coefficients Y_l^{Mij} does not pose a problem provided that each grid cell is assigned an integer number representing a type of material cell (a set of material parameters) and the heterogeneity of the medium is de-

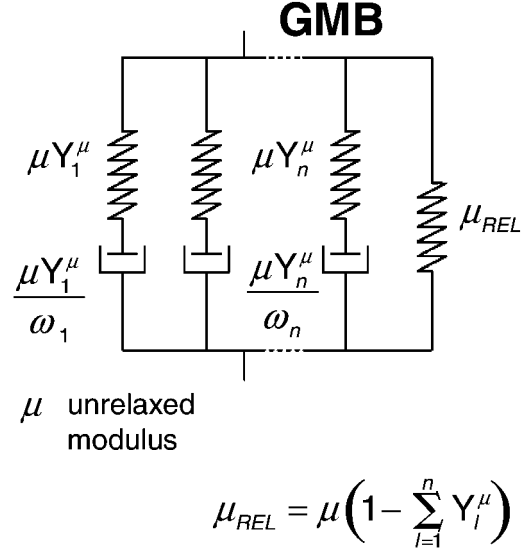


Figure 1. Generalized Maxwell body representing a complex viscoelastic torsion modulus with elastic moduli μY_l^μ , viscosities $\mu Y_l^\mu / \omega_l$, and relaxed modulus μ_{REL} . An analogous body is assumed for a complex viscoelastic bulk modulus.

scribed as a spatial distribution of types of material cells. What is desirable to reduce is the number of the anelastic functions ζ_l^{ij} in the whole grid. Zeng (1996), Day (1998), and Day and Bradley (2001) developed approaches allowing coarse spatial sampling of the anelastic functions. In Day's (1998) approach, one anelastic function ζ_l^{ij} for one relaxation frequency ω_l is distributed with a spatial period of $2h$, h being a grid spacing. Consequently, $n = 8$. Considering, for example, location of the stress-tensor component T_{zx} at eight corners of a grid cube $h \times h \times h$, only one of the eight ζ_l^{zx} anelastic functions is assigned to one of the eighth corners (say, ζ_1^{zx} is assigned to one position, ζ_2^{zx} to other position, and so on). Consequently, the total number of ζ_l^{zx} , $l = 1, 2, \dots, 8$, in the whole grid is $MX/2 \cdot MY/2 \cdot MZ/2 \cdot 8 = MX \cdot MY \cdot MZ$. Because we have six independent stress-tensor components, the total number of all anelastic functions in the whole grid is $MX \cdot MY \cdot MZ \cdot 6$. Because the anelastic coefficients Y_l^{Mij} are distributed in the same manner, the total number of all the anelastic coefficients in the whole grid is $MX \cdot MY \cdot MZ \cdot 5$. Thus, the additional memory due to attenuation in Day's (1998) approach in the displacement-stress or displacement-velocity-stress or velocity-stress scheme, compared with equation (10), is

$$N^{\text{additional}} = p \cdot MX \cdot MY \cdot MZ \cdot 11. \quad (11)$$

It is clear from equations (10) and (11) that the additional memory in the case of eight relaxation frequencies is equivalent to the case of just one relaxation frequency in Emmerich and Korn's (1987) original treatment, which is significant.

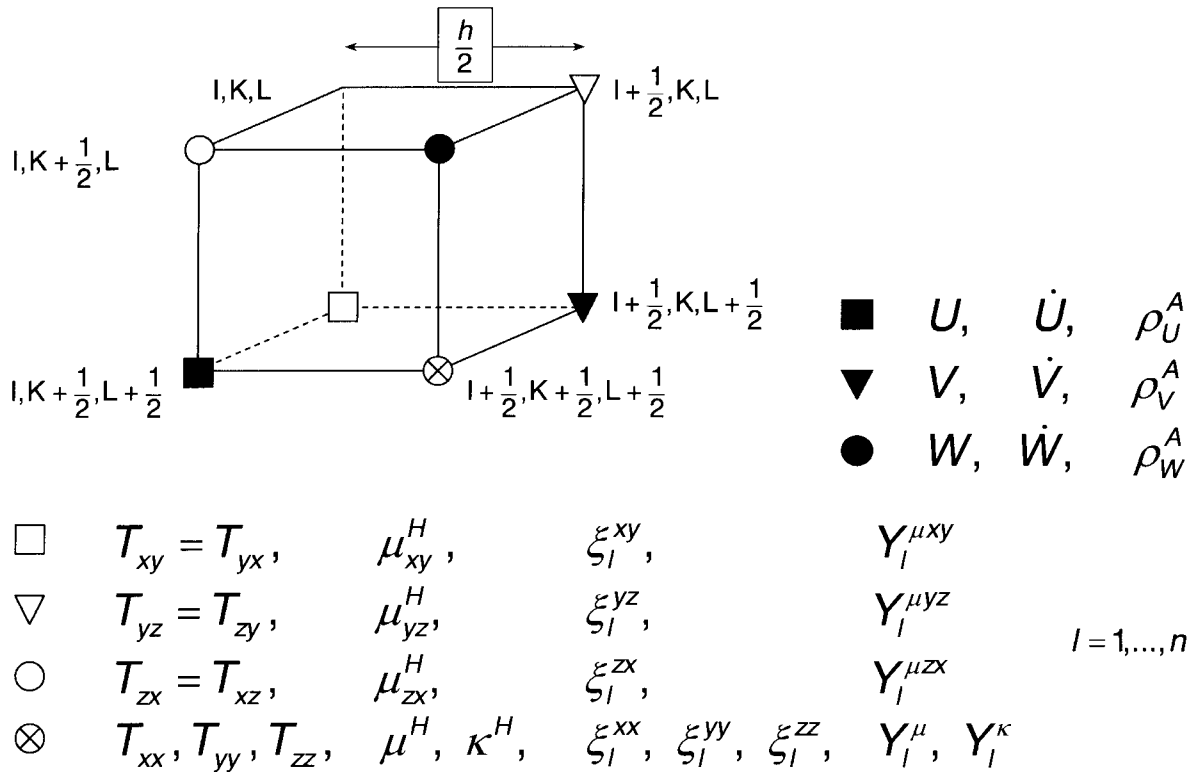


Figure 2. A staggered-grid FD cell with positions of the wave-field variables (displacement and/or velocity vector components, stress-tensor components, and anelastic functions) and effective media parameters (elastic bulk and shear moduli, and anelastic coefficients; indices A and H indicate, e.g., arithmetic and harmonic averages as defined in Moczo *et al.* [2002]).

Incorporation of Attenuation in Media with Material Discontinuities

Heterogeneous FD Schemes

Realistic models of the Earth’s interior often have to include layers/blocks of different materials, and thus also interfaces (material discontinuities) between them, at which material parameters change discontinuously. The equation of motion governs the motion outside the discontinuity, but boundary conditions (for example, continuity of displacement and traction vectors at welded interfaces) apply to the discontinuity. In the heterogeneous approach only one FD scheme is used for all interior grid points (points not lying on boundaries of a grid) regardless of their positions with respect to the discontinuity. The presence of the discontinuity is accounted for only by values of (effective) grid material parameters.

Justification and construction of heterogeneous FD schemes has recently been addressed by Moczo *et al.* (2002), who analyzed 1D and 3D elastic problems. In the 1D problem for a welded planar interface, they found a simple physical model of the contact of two media and the exact heterogeneous formulation of the equation of motion and Hooke’s law, that is, equations for an averaged medium representing the contact. Then they constructed a corresponding 1D het-

erogeneous FD scheme. In the 3D problem, they analyzed three cases: (1) a planar interface parallel to a coordinate plane in the Cartesian coordinate system, (2) a planar interface in a general position, and (3) a nonplanar interface between two isotropic media. In case 1, the averaged medium representing the planar-interface contact of two isotropic media is transversally isotropic: five independent elastic coefficients describe the averaged medium, that is, Hooke’s law includes five independent elastic coefficients. In case 2, 21 generally nonzero elastic coefficients are necessary to describe the averaged medium at a point of the interface. The same is true for case 3 assuming that a tangential planar interface is used at a point to approximate the nonplanar interface. Because a corresponding heterogeneous FD scheme would require tremendous computer memory, they considered simplified boundary conditions at the contact for which the averaged medium is described by only two elastic coefficients, as any of the two isotropic media in contact. Based on the simplified approach, Moczo *et al.* (2002) constructed the explicit heterogeneous 3D fourth-order in space, second-order in time, staggered-grid FD scheme with volume harmonic averaging of the bulk and shear moduli and volume arithmetic averaging of density. As documented by accuracy tests, the scheme allows for an arbitrary position of the discontinuity in the spatial grid. The scheme can account

for a difference in a layer thickness smaller than the spatial grid spacing. Moczo *et al.* (2002) demonstrated that such a thickness variation can yield a considerably different seismic motion. (This is an important supportive argument for the approach presented later.) The structure of the scheme is the same as that of standard fourth-order staggered-grid FD schemes. The difference lies in the definition of the grid material parameters. Referring to Figure 2, a volume arithmetic average of density and volume harmonic averages of elastic moduli are evaluated as

$$\rho_{l,K+\frac{1}{2},L+\frac{1}{2}}^A = \frac{1}{h^3} \int_{x_{l-1/2}}^{x_{l+1/2}} \int_{y_K}^{y_{K+1}} \int_{z_L}^{z_{L+1}} \rho dx dy dz, \quad (12)$$

$$\kappa_{l+\frac{1}{2},K+\frac{1}{2},L+\frac{1}{2}}^H = \left[\frac{1}{h^3} \int_{x_l}^{x_{l+1}} \int_{y_K}^{y_{K+1}} \int_{z_L}^{z_{L+1}} \frac{1}{\kappa} dx dy dz \right]^{-1}, \quad (13)$$

$$\mu_{l+\frac{1}{2},K+\frac{1}{2},L+\frac{1}{2}}^H = \left[\frac{1}{h^3} \int_{x_l}^{x_{l+1}} \int_{y_K}^{y_{K+1}} \int_{z_L}^{z_{L+1}} \frac{1}{\mu} dx dy dz \right]^{-1}. \quad (14)$$

Contact of Two Viscoelastic Media

Each of the two viscoelastic media is described by real density and complex frequency-dependent bulk and shear moduli given, in the case of the GMB rheology, by equation (6). As is clear from equations (7) and (8), the question is how to determine elastic (unrelaxed) moduli and anelastic coefficients for an averaged medium representing a contact of two media if a material discontinuity goes through a grid cell. Applying averaging (for example, volume harmonic averages-equations 13 and 14) to viscoelastic moduli, we can numerically determine average viscoelastic moduli in the frequency domain. Having the averaged viscoelastic moduli, we can determine the corresponding quality factors:

$$\bar{Q}_M^{-1}(\bar{\omega}_k) = \text{Im } M_n^A(\bar{\omega}_k) / \text{Re } M_n^A(\bar{\omega}_k); \quad (15)$$

$$k = 1, 2, \dots, 2n - 1.$$

Assuming that the rheology of the averaged medium can be approximated by the GMB rheology, we can use a system of equations analogous to equations (4) to determine anelastic coefficients corresponding to the averaged medium.

It is clear from equation (6) that $M_U = \lim_{\omega \rightarrow \infty} M_n(\omega)$. An obvious implication is that the limit taken from the averaged viscoelastic modulus gives the averaged unrelaxed (elastic) modulus. In other words, the elastic moduli of the averaged viscoelastic medium can be obtained in the same way as in the perfectly elastic medium (for example, using formulas 13 and 14 for elastic moduli).

Contact of Two Media and Day's Coarse Graining

While Day's (1998) coarse spatial distribution and its recent improvement by Graves and Day (2003) are excellent tools to make the viscoelastic calculation in smoothly heterogeneous medium efficient, it is clear that an interface between two media may be so localized that the two media are characterized in two disjunctive (not overlapping) frequency intervals. Then, how can the two media physically interact and be averaged? In principle, it would be possible at one grid position to account also for neighboring functions (and thus relaxation frequencies) by including properly weighted anelastic functions from neighboring grid positions in the sum of the functions in equation (7). This, however, is not a good solution because it would introduce artificial additional smoothing (averaging) of material parameters. The reason is that the anelastic functions defined by equations (8) depend on the anelastic coefficients.

New Definition of Anelastic Functions

In order to overcome the limitation discussed earlier and, at the same time, keep coarse spatial sampling, it is necessary to define anelastic functions in a new way and rewrite Hooke's law for the viscoelastic medium accordingly. If we divide each equation of the system of equations (3) by an appropriate anelastic coefficient Y_l^M and define new anelastic functions as

$$\zeta_l^{\text{new},ij} = \zeta_l^{M,ij} / Y_l^M, \quad (16)$$

the system (3) of $9n$ equations becomes a system,

$$\zeta_l^{\text{new},ij} + \omega_l \zeta_l^{\text{new},ij} = \omega_l \varepsilon_{ij}; \quad (17)$$

$$l = 1, 2, \dots, n; i, j \in \{1, 2, 3\},$$

of $6n$ independent equations. It is clear from system (17) that the new anelastic functions do not depend on the material properties, that is, on anelastic coefficients. Inserting definition (16) into equation (2) leads to Hooke's law in the form

$$\tau_{ij} = \kappa \varepsilon_{kk} \delta_{ij} + 2\mu (\varepsilon_{ij} - \frac{1}{3} \varepsilon_{kk} \delta_{ij})$$

$$- \sum_{l=1}^n [\kappa Y_l^k \zeta_l^{\text{new},kk} \delta_{ij} + 2\mu Y_l^i (\zeta_l^{\text{new},ij} - \frac{1}{3} \zeta_l^{\text{new},kk} \delta_{ij})]. \quad (18)$$

Implementation in the Staggered-Grid FD Scheme

Time-Integration Scheme

With the second-order accuracy, $\zeta_l^{\text{new},ij}$ may be approximated by a central-difference formula and the anelastic function itself by

$$\zeta_l^{\text{new},ij}(t_m) = (\zeta_l^{\text{new},ij}(t_{m-1/2}) + \zeta_l^{\text{new},ij}(t_{m+1/2}))/2, \quad (19)$$

where t_m denotes the m th time level. Then it follows from system (17) that

$$\zeta_l^{\text{new},ij}(t_{m+1/2}) = \frac{2\omega_l\Delta t}{2 + \omega_l\Delta t} \varepsilon_{ij}(t_m) + \frac{2 - \omega_l\Delta t}{2 + \omega_l\Delta t} \zeta_l^{\text{new},ij}(t_{m-1/2}), \quad (20)$$

where Δt is a timestep. Obviously, the value of $\zeta_l^{\text{new},ij}(t_m)$ calculated using schemes (19) and (20) may be used in a FD scheme solving equation (18). It is, however, possible to avoid the necessity to keep in memory both $\zeta_l^{\text{new},ij}(t_{m-1/2})$ and $\zeta_l^{\text{new},ij}(t_{m+1/2})$ for a grid position at one time by inserting equation (20) into equation (19) and obtaining

$$\zeta_l^{\text{new},ij}(t_m) = -\frac{\omega_l\Delta t}{2 - \omega_l\Delta t} \varepsilon_{ij}(t_m) + \frac{2}{2 - \omega_l\Delta t} \zeta_l^{\text{new},ij}(t_{m+1/2}). \quad (21)$$

Insertion of equation (21) into Hooke's law (equation 18) and rearranging gives

$$\tau_{ij}(t_m) = \tilde{\kappa}\varepsilon_{kk}(t_m)\delta_{ij} + 2\tilde{\mu}(\varepsilon_{ij}(t_m) - \frac{1}{3}\varepsilon_{kk}(t_m)\delta_{ij}) - \sum_{l=1}^n [\tilde{Y}_l^\kappa \zeta_l^{\text{new},kk}(t_{m+1/2})\delta_{ij} + 2\tilde{Y}_l^\mu (\zeta_l^{\text{new},ij}(t_{m+1/2}) - \frac{1}{3}\zeta_l^{\text{new},kk}(t_{m+1/2})\delta_{ij})], \quad (22)$$

where

$$\begin{aligned} \tilde{\kappa} &= \kappa \left(1 + \sum_{l=1}^n d_l Y_l^\kappa \right), & \tilde{\mu} &= \mu \left(1 + \sum_{l=1}^n d_l Y_l^\mu \right) \\ \tilde{Y}_l^\kappa &= c_l \kappa Y_l^\kappa, & \tilde{Y}_l^\mu &= c_l \mu Y_l^\mu \\ d_l &= \frac{\omega_l \Delta t}{2 - \omega_l \Delta t}, & c_l &= \frac{2}{2 - \omega_l \Delta t}. \end{aligned} \quad (23)$$

We can see that using scheme (20) and a proper scheme for equation (22), it is enough to have only one variable for one anelastic function at one grid position at any time.

Spatial Distribution of Anelastic Coefficients and Functions

As stated earlier, the spatial distribution of the anelastic coefficients shown in Figure 2 does not pose a memory problem if each grid cell is assigned an integer number representing a type of material cell and the heterogeneity of the medium is described as a spatial distribution of the types of material cells. Such an approach is not a new one. It has been advantageously applied, for example, by Kristek *et al.* (1999) to model seismic motion in the Osaka sedimentary basin with a complex shape of the sediment–basement interface. Moczo *et al.* (2002) demonstrated considerable dif-

ferences in seismic motions due to variations in layer thickness smaller than the spatial grid spacing (taken as 1/6 of the minimum wavelength). This means that it can be important to account for the heterogeneity of the medium inside a grid cell. Thus, in our implementation, each grid cell contains $Y_l^\kappa, Y_l^\mu, Y_l^{\mu xy}, Y_l^{\mu yz}, Y_l^{\mu zx}, l = 1, 2, \dots, n$.

With the new anelastic functions, independent of anelastic coefficients, it is possible to define their coarse spatial distribution different from that of Day's (1998). Figure 3 shows a natural choice of the number of the relaxation frequencies, $n = 4$, and the spatial distribution of the anelastic functions. One grid cell contains all anelastic functions for one relaxation frequency. As it is clear from Figure 3, the total number of the all anelastic functions in the whole grid is $2 \cdot MX/2 \cdot MY/2 \cdot MZ/2 \cdot 6 \cdot 4 = MX \cdot MY \cdot MZ \cdot 6$, the same as in Day's (1998) approach. Because, as explained earlier, the number of the anelastic coefficients does not pose a memory problem, we keep all $Y_l^\kappa, Y_l^\mu, Y_l^{\mu xy}, Y_l^{\mu yz}, Y_l^{\mu zx}, l = 1, \dots, 4$, in each grid cell.

Accounting for All Relaxation Frequencies and Functions at a Grid Position

Let $T_{I,K,L}$ be any of the shear stress-tensor components in grid cell (I,K,L) . Then, omitting the time index, a FD scheme for equation (22) may be symbolically written as

$$T_{I,K,L} = 2\tilde{\mu}_{I,K,L} E_{I,K,L} - 2 \sum_{l_{\text{REL}}=1}^4 \tilde{Y}_{l_{\text{REL}},I,K,L} X_{l_{\text{REL}},I,K,L}.$$

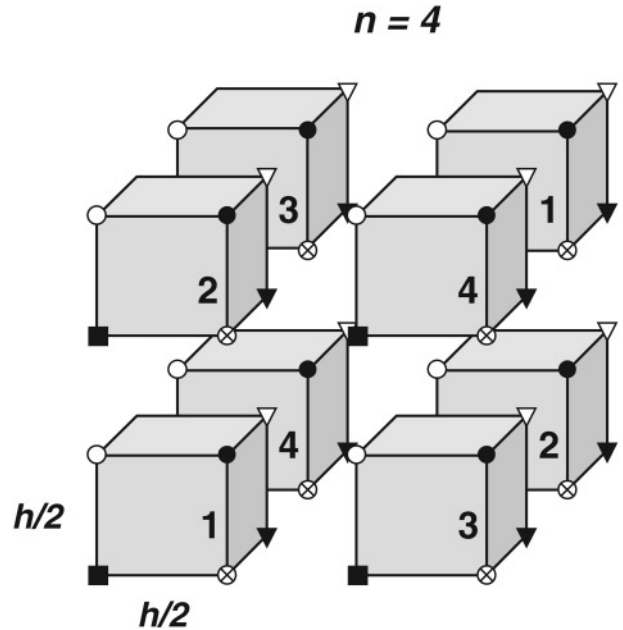


Figure 3. Spatial distribution of grid cells and anelastic functions. The number on a cell face indicates the relaxation frequency for which the anelastic functions are localized in the cell. For example, grid cell 1 contains $\zeta_1^{\text{new},xx}, \zeta_1^{\text{new},yy}, \zeta_1^{\text{new},zz}, \zeta_1^{\text{new},xy}, \zeta_1^{\text{new},yz}, \zeta_1^{\text{new},zx}$, and so on.

Because in a particular grid cell (I,K,L) the anelastic function only for one particular relaxation frequency is available, we can approximate the sum over $l = 1, \dots, 4$ by weighted averaging of the anelastic functions from the grid cell (I,K,L) and neighboring grid cells. The scheme

$$T_{I,K,L} = 2\tilde{\mu}_{I,K,L}E_{I,K,L} - 2\tilde{Y}_{\text{ind}(I,K,L);I,K,L} \cdot X_{\text{ind}(I,K,L);I,K,L} - 2\tilde{Y}_{\text{ind}(I-1,K,L);I,K,L} \cdot \frac{X_{\text{ind}(I-1,K,L);I-1,K,L} + X_{\text{ind}(I+1,K,L);I+1,K,L}}{2} - 2\tilde{Y}_{\text{ind}(I,K-1,L);I,K,L} \cdot \frac{X_{\text{ind}(I,K-1,L);I,K-1,L} + X_{\text{ind}(I,K+1,L);I,K+1,L}}{2} - 2\tilde{Y}_{\text{ind}(I,K,L-1);I,K,L} \cdot \frac{X_{\text{ind}(I,K,L-1);I,K,L-1} + X_{\text{ind}(I,K,L+1);I,K,L+1}}{2}$$

with

$$\text{ind}(I,K,L) = (K \bmod 2) \cdot \{1 + (L-1) \bmod 2 + 2[(I-1) \bmod 2]\} = (1 - K \bmod 2) \cdot \{1 + (L) \bmod 2 + 2[(I) \bmod 2]\}$$

gives natural averaging in three coordinate directions. An analogous but longer formula is easily obtained for the normal stress-tensor components.

Numerical Tests

Two models of a single layer over half-space are schematically shown in Figure 4. In model M1, the layer–half-space interface is located at a grid plane with the shear stress-tensor components; in model M2, it is at a grid plane with the normal stress-tensor components. The model parameters are in Table 1. Futterman’s (1962) $Q(\omega)$ law was assumed. A double-couple point source (0 m, 0 m, 525 m) was simulated using a body-force term, and its source-time function was the Gabor signal, $s(t) = \exp\{-[\omega(t - t_s)/\gamma]^2\} \cos[\omega(t - t_s) + \theta]$, $\omega = 2\pi f_p$, $t \in \langle 0, 2t_s \rangle$. Here, f_p is the predominant frequency, γ controls the width of the signal, θ is a phase shift, and $t_s = 0.45\gamma/f_p$. The source parameters are in Table 2. A receiver’s coordinates were (1475 m, 0 m, 25 m). The numbers of grid cells in the x , y and z directions were $MX = 301$, $MY = 301$, and $MZ = 402$. The grid spacing was $h = 50$ m, timestep $\Delta t = 0.0045$ sec. Except for the inclusion of the attenuation, the FD calculation (elastic part of the scheme, point source simulation, free surface, non-reflecting boundaries) is the same as in Moczo *et al.* (2002).

For both M1 and M2 models, synthetics were calculated using our approach, using Day and Bradley’s (2001) approach, and by the discrete-wavenumber (DWN) method (Bouchon, 1981; computer code Axitra by Coutant, 1989). All synthetics are compared in Figure 5. We can see that the synthetics obtained by our approach are in better agreement with the DWN method than those obtained by Day and Bradley’s (2001) approach.

Table 1

Model Parameters: Surface Layer over Half-Space

Both Models, M1 and M2	α (m/sec)	β (m/sec)	ρ (kg/m ³)	Q_p (1 Hz)	Q_s (1 Hz)
Layer	1125	625	1600	10	5
Half-space	5468	3126	1800	100	50

Layer thickness: M1, 200 m; M2, 225 m. α , P -wave velocity; β , S -wave velocity; ρ , density.

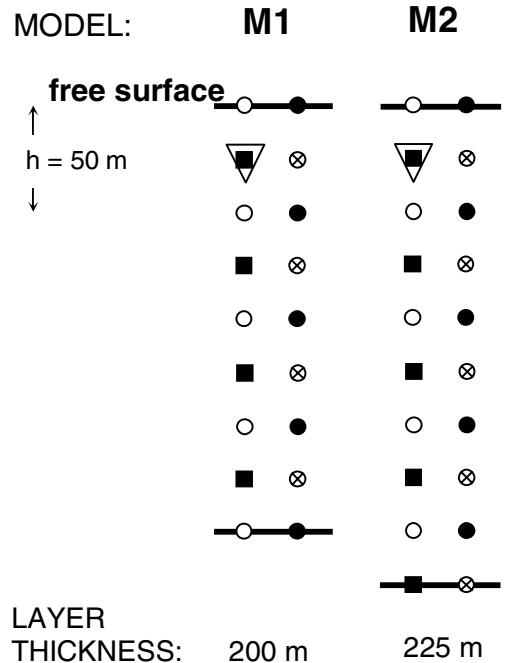
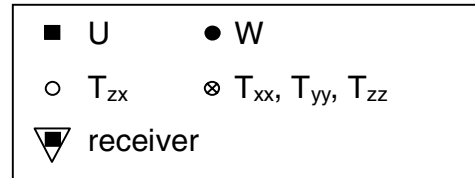


Figure 4. Positions of the free surface and layer–half-space interface in two models of a surface layer over half-space, shown schematically in one vertical grid plane. M1 and M2 differ in the position of the layer–half-space interface in the spatial grid (the same for both models) and thus in the layer thickness; the difference in thickness is equal to half grid spacing. Parameters of the model are in Table 1.

Table 2
Source Parameters

M_0 (N m)	ϕ_s (deg)	δ (deg)	λ (deg)	γ	f_p	θ	t_s
10^{16}	0	45	90	1.5	0.225	$\pi/2$	3.0

M_0 (N m), seismic moment; ϕ_s , strike; δ , dip; λ , rake; γ , f_p , θ , and t_s , parameters of Gabor signal.

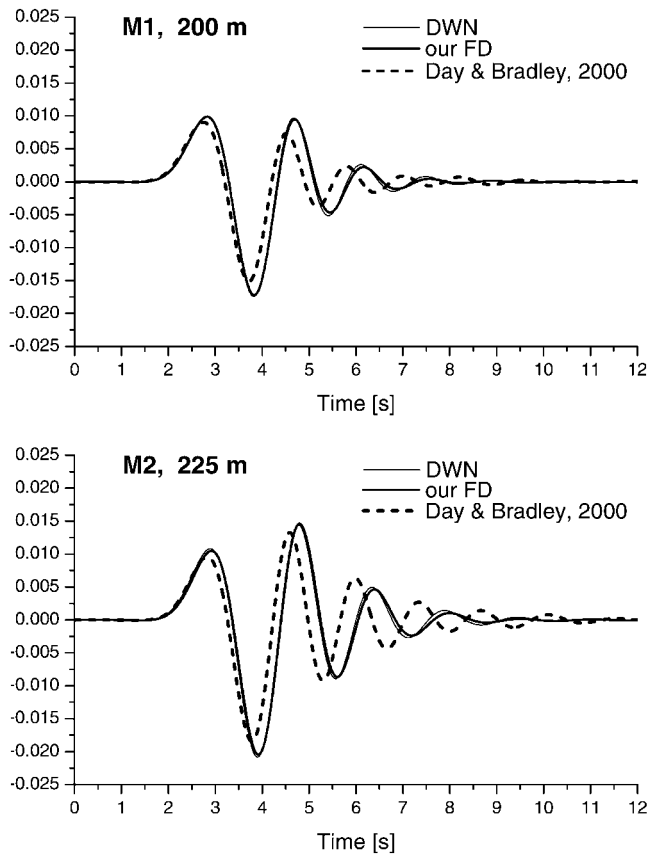


Figure 5. Comparison of synthetics obtained by our approach and Day and Bradley's approach with discrete-wavenumber (DWN) synthetics for models M1 and M2. Note the very good accuracy of our FD synthetics for both positions of the layer-half-space interface with respect to the spatial grid. Also note the considerable difference between synthetics due to variation in the layer thickness equal to half grid spacing.

Conclusions

We briefly reviewed the incorporation of realistic attenuation into time-domain computations of seismic-wave propagation with an emphasis on computational efficiency. We considered the problem of accounting for a material discontinuity in heterogeneous FD schemes for perfectly elastic and viscoelastic media. We showed that the anelastic coefficients and elastic moduli of the averaged medium representing contact of two media can be determined from averaging applied to viscoelastic and elastic moduli, respectively.

In order to account properly for material discontinuities and, at the same time, be memory efficient, we defined (1) the anelastic functions in a new way, as being independent of anelastic coefficients (that is, independent of material parameters), and (2) a new coarse spatial distribution of the anelastic functions. As a consequence, in the sum of the anelastic functions in Hooke's law we can, at a given grid position, account for anelastic functions at neighboring grid positions (and thus for other relaxation frequencies) by proper weighted averaging of the anelastic functions from neighboring grid positions without artificial additional averaging of the material parameters themselves.

If the anelastic functions are determined from volume harmonic averages of the viscoelastic moduli, we get a consistent extension of the recently developed elastic FD scheme (Moczo *et al.*, 2002), which was shown to be more accurate for media with discontinuities than standard staggered-grid FD schemes. Numerical tests demonstrate that our approach enables more accurate viscoelastic modeling than other approaches.

Acknowledgments

This work was supported in part by Grant Number 2/1090/21, VEGA, Slovak Republic, European Commission Project Numbers EVG1-CT-2000-00026 SESAME and EVG1-CT-2001-00040 EUROSEISRISK. Comments by an anonymous reviewer helped to improve the article.

References

- Bouchon, M. (1981). A simple method to calculate Green's functions for elastic layered media, *Bull. Seism. Soc. Am.* **71**, 959–971.
- Carcione, J. M., D. Kosloff, and R. Kosloff (1988). Wave propagation simulation in a linear viscoelastic medium, *Geophys. J. R. Astr. Soc.* **95**, 597–611.
- Coutant, O. (1989). Program of numerical simulation AXITRA, Res. Rep. LGIT, Université Joseph Fourier, Grenoble (in French).
- Day, S. M. (1998). Efficient simulation of constant Q using coarse-grained memory variables, *Bull. Seism. Soc. Am.* **88**, 1051–1062.
- Day, S. M., and C. R. Bradley (2001). Memory-efficient simulation of anelastic wave propagation, *Bull. Seism. Soc. Am.* **91**, 520–531.
- Day, S. M., and J. B. Minster (1984). Numerical simulation of wavefields using a Padé approximant method, *Geophys. J. R. Astr. Soc.* **78**, 105–118.
- Emmerich, H., and M. Korn (1987). Incorporation of attenuation into time-domain computations of seismic wave fields, *Geophysics* **52**, 1252–1264.
- Futterman, W. I. (1962). Dispersive body waves, *J. Geophys. Res.* **67**, 5279–5291.
- Graves, R. W. (1996). Simulating seismic wave propagation in 3D elastic media using staggered-grid finite differences, *Bull. Seism. Soc. Am.* **86**, 1091–1106.
- Graves, R. W., and S. M. Day (2003). Stability and accuracy analysis of coarse-grain viscoelastic simulations, *Bull. Seism. Soc. Am.* **93**, 283–300.
- Kristek, J., P. Moczo, I. Irikura, T. Iwata, and H. Sekiguchi (1999). The 1995 Kobe mainshock simulated by the 3D finite differences, in *The Effects of Surface Geology on Seismic Motion*, K. Irikura, K. Kudo, H. Okada, and T. Sasatani (Editors), Vol. 3, Balkema, Rotterdam, 1361–1368.

- Moczo, P., E. Bystrický, J. Kristek, J. M. Carcione, and M. Bouchon (1997). Hybrid modelling of *P-SV* seismic motion at inhomogeneous viscoelastic topographic structures, *Bull. Seism. Soc. Am.* **87**, 1305–1323.
- Moczo, P., J. Kristek, and E. Bystrický (2001). Efficiency and optimization of the 3D finite-difference modeling of seismic ground motion, *J. Comp. Acoustics* **9**, 593–609.
- Moczo, P., J. Kristek, V. Vavryčuk, R. J. Archuleta, and L. Halada (2002). 3D heterogeneous staggered-grid finite-difference modeling of seismic motion with volume harmonic and arithmetic averaging of elastic moduli and densities, *Bull. Seism. Soc. Am.* **92**, 3042–3066.
- Zeng, X. (1996). Finite difference modeling of viscoelastic wave propagation in a generally heterogeneous medium in the time domain, and a dissection method in the frequency domain, *Ph.D. Thesis*, University of Toronto.

Geophysical Institute
Slovak Academy of Sciences
Dúbravská cesta 9
845 28 Bratislava, Slovak Republic
(J.K.)

Department of Physics of the Earth and Planets
Faculty of Mathematics, Physics, and Informatics
Comenius University
Mlynská dolina F1
842 48 Bratislava, Slovak Republic
(P.M.)

Manuscript received 23 January 2003.